Exp Brain Res (2015) 233:657–669
DOI 10.1007/s00221-014-4145-0

RESEARCH ARTICLE

The influence of visual information on multi-muscle control during quiet stance: a spectral analysis approach

Alessander Danna-Dos-Santos · Adriana M. Degani · Tjeerd W. Boonstra · Luis Mochizuki · Allison M. Harney · Megan M. Schmeckpeper · Lori C. Tabor · Charles T. Leonard

Received: 6 May 2014 / Accepted: 7 November 2014 / Published online: 19 November 2014

Abstract Standing upright requires the coordination of neural drives to a large set of muscles involved in controlling human bipedal stance (i.e., postural muscles). The coordination may deteriorate in situations where standing is performed under more challenging circumstances, such as standing on a smaller base of support or not having adequate visual information. The present study investigates the role of common neural inputs in the organization of multi-muscle synergies and the effects of visual input disruption to this mechanism of control. We analyzed the strength and distribution of correlated neural inputs (measured by intermuscular coherence) to six postural muscles previously recognized as components of synergistic groups involved in the maintenance of the body's vertical positioning. Two experimental conditions were studied: quiet bipedal stance performed with opened eyes (OEs) and closed eyes (CEs). Nine participants stood quietly for 30 s while the activity of the soleus, biceps femoris, lumbar erector spinae, tibialis anterior, rectus femoris, and rectus abdominis muscles were recorded using surface electrodes. Intermuscular (EMG–EMG) coherence was estimated for 12 muscle pairs formed by these muscles, including pairs formed solely by either posterior, anterior, or mixed (one posterior and one anterior) muscles. Intermuscular coherence was only found to be significant for muscle pairs formed solely by either posterior or anterior muscles, and no significant coherence was found for mixed muscle pairs. Significant intermuscular coherence was only found within a distinct frequency interval bounded between 1 and 10 Hz when visual input was available (OEs trials). The strength of correlated neural inputs was similar across muscle pairs located in different joints but executing a similar function (pushing body either backward or forward) suggesting that synergistic postural groups are likely formed based on their functional role instead of their anatomical location. Absence of visual information caused a significant decrease in intermuscular coherence. These findings are consistent with the hypothesis that correlated neural inputs are a mechanism used by the CNS to assemble synergistic muscle groups. Further, this mechanism is affected by interruption of visual input.

Keywords Synergy · Posture · Muscle mode · Vision · Electromyogram · Intermuscular coherence

A. Danna-Dos-Santos (✉) · A. M. Degani · A. M. Harney · M. M. Schmeckpeper · L. C. Tabor · C. T. Leonard
School of Physical Therapy and Rehabilitation Science, University of Montana, 32 Campus Drive, 135 Skaggs Building, Missoula, MT 59812-4680, USA
e-mail: alex.santos@umontana.edu

T. W. Boonstra
School of Psychiatry, University of New South Wales, Sydney, Australia

T. W. Boonstra
Black Dog Institute, Sydney, Australia

T. W. Boonstra
MOVE Research Institute, VU University, Amsterdam, The Netherlands

L. Mochizuki
School of Arts, Sciences and Humanities, University of Sao Paulo, São Paulo, Brazil

Introduction

Execution of the bipedal stance posture involves many mechanical challenges imposed by the design of our skeletal system. For example, the vertical orientation of the head–leg–trunk segments, the high center of mass, the

large number of joints, and the narrow base of support all introduce mechanical instability that needs to be counterbalanced by the precise activation of multiple muscles spanning across multiple joints (ankle, knee, hip, and intervertebral joints). Therefore, the central nervous system (CNS) is posed with the task of coordinating the activation of all these muscles.

Previous studies have provided important insights into the principles of multi-muscle control, including evidence that the CNS unites muscles into functional groups (synergists) to reduce the number of control variables and to use these muscle groups as the basic elements of control (Bernstein 1967, reviewed in Latash 2008). According to this perspective, the control of the human bipedal stance can be represented by a hierarchical scheme composed of at least two levels: a lower level where these functional groups are formed and a higher level where these groups are activated in a synergistic fashion to control physical variables directly related to task execution (Latash 2008). Several experimental findings support this proposition: For example, Krishnamurthy et al. (2003a) reported that during the execution of vertical stance associated with a whole-body voluntary sway, three major functional muscle groups co-varied their magnitude to provide a stable trajectory of the position of the body's center of pressure (COP). These authors used principal component analysis to identify these muscle groups and introduced the term *muscle mode* (or M-mode) to describe them. One may view M-modes as "virtual muscles" that are manipulated at a higher level of the control hierarchy for the control of relevant task variables. The M-modes identified were as follows: a posterior M-mode formed by posterior postural muscles (soleus, biceps femoris, semi tendinous, lumbar erector spinae, and gastrocnemius), an anterior M-mode formed by anterior postural muscles (tibialis anterior, vastus medial's, vastus lateralis, rectus femoris, and rectus abdominis muscle), and a third M-mode often formed solely by the rectus abdominis muscle (Krishnamurthy et al. 2003a). These findings have been replicated by others, although the neural mechanisms related to their formation remain unclear (Krishnamurthy 2003b; Wang et al. 2005; Danna-dos-Santos et al. 2007, 2008, 2009).

Recently, we investigated the role of correlated neural inputs as a neural mechanism by which the CNS coordinates the activation of synergistic muscles forming only one of these M-modes (Danna-dos-Santos et al. 2014). More specifically, we employed measures of intermuscular coherence between pairs of EMG signals composing the posterior M-mode (soleus, biceps femoris, and lumbar erector spinae muscles) and confirmed the presence of correlated neural inputs to all three muscles. In order to further understand this mechanism, investigations involving additional muscles and experimental conditions are still necessary.

The first goal of the present study was to expand our previous investigations and include the analysis of both anterior and posterior M-modes (two major synergistic groups involved in quiet standing control). It was only by the inclusion of an additional major M-mode that allowed us to investigate the role of common neural inputs in the formation of multi-muscle synergistic groups. We hypothesized that muscles comprising each of these synergistic groups would be coordinated by correlated neural inputs (Gibbs et al. 1995) and hence will exhibit significant values of intermuscular coherence.

The second goal was to investigate the effect of visual information on intermuscular coherence. Visual information contributes considerably to the control of bipedal stance; e.g., poor or absent visual input has a detrimental effect on postural stability (Allum and Pfaltz 1985; Fitzpatrick et al. 1992; Simoneau et al. 1992; Schumann et al. 1995; Wood et al. 2009) and manipulation of the visual environment mimicking motion of the visual environment can induce changes to the dynamics of postural sway (Lee and Lishman 1975; Schöner 1991; Dijkstra et al. 1994a, b; Polastri and Barela 2013; Barela et al. 2014). In the absence of vision, intermuscular coherence at 0–5 Hz between bilateral leg muscles was reduced during quiet standing (Boonstra et al. 2008). Here, we investigate the absence of visual input interferes with the generation of common neural inputs to muscles forming the anterior and posterior synergistic groups reported by Krishnamurthy et al. (2003a). We expect that a disruption of visual information will result in a significant reduction of correlated neural inputs, leading to significantly reduced intermuscular coherence across synergistic muscles.

Methods

Participants

Nine healthy adults (5 females and 4 males, 26.0 ± 2.7 years, 175.8 ± 13.2 cm height, 81.7 ± 22.8 kg weight) participated voluntarily in this study. All participants were healthy and had no history of neurological or muscular disorder. All participants were right-handed and right-footed based on their preferred hand for writing and eating, and foot for kicking a soccer ball. Prior to participation, all participants voluntarily gave their informed consent based on the procedures approved by the Institutional Review Board at The University of Montana and conformed to The Declaration of Helsinki.

Apparatus

A force platform (AMTI BP400600, AMTI Inc.) was used to acquire the body's COP coordinates in anterior–posterior

(COPap) and medial–lateral directions (COPml). Features of the COP were included on this study due to its relation to low-frequency EMG modulation (Gatev et al. 1999; Mochizuki et al. 2006).

Active surface electrodes (Delsys Bagnoli single differential DE-2.1) were used to record the activity of the following muscles: soleus (SOL), biceps femoris (BF), lumbar erector spinae (ERE), tibialis anterior (TA), rectus femoris (RF), and rectus abdominis (RA). These electrodes were placed on the right side of the body over the muscle bellies according to Criswell (2010) and in a similar fashion to previous studies (Danna-dos-Santos et al. 2007, 2008, 2014). The distance between electrode pairs was kept at 1 cm, and a total area of surface recording was of 10 mm^2 for each electrode. A reference electrode was placed over the lateral aspect of the left fibular malleolus. EMG signals were amplified (1,000×) and band-pass filtered (6–500 Hz). All signals were sampled at 1.2 kHz with a 12-bit resolution.

Experimental procedures

All participants performed four independent quiet standing trials. Two trials were performed with opened eyes (OEs) and two with closed eyes (CE). To avoid any possible effects of CE trials on the distribution of common neural inputs recorded during OEs trials, OEs trials were performed first. During OEs trials, participants were instructed to stand on the force platform with their feet parallel and 15 cm apart. The position of the feet was determined, so the center of the base of support area was closely aligned with the center of the force plate surface. To avoid any discrepancies between feet positioning across trials, the initial feet position was marked on the top of the platform and subjects were asked not to move their feet during the entire data recording (approximately 6 min). Participants were instructed to cross their upper limbs against the chest and focus their vision to a physical static point placed at eyes height and at a distance of approximately 2 m. Once participants were in this position, they were asked to remain steady for 35 s keeping their body as vertical as possible and to distribute their body weight evenly between the two feet. Equal distribution of the weight was verified on-line by the investigators (via force plate feedback available only to research personnel). To avoid recording of any transient effects, the first 5 s were discarded and the remaining 30 s were analyzed. Participants were barefoot during the entire experiment. An inter-trial interval of 60 s was provided for participants to relax and change position. The total duration of the experiment, including preparation and placement of electrodes, explanation of the task, and data recording was approximately 25 min and none of the participants reported fatigue as an issue.

Data processing

All signals recorded (COP and EMG signals) were analyzed off-line with custom-written software routines (Matlab R2012b, The MathWorks). COPap and COPml coordinate signals were filtered with a 20-Hz low-pass, second-order, and zero-lag Butterworth filter before further processing. All COP coordinates were normalized by subtracting COP signals from its average position calculated over the 30-s recording time.

Analysis of COP behavior

The elliptical area containing 95 % of the COP path (*Area*), and the ranges, and mean velocities in both directions (*Range COPap, Range COPml, MVCOPap*, and *MVCOPml*, respectively) were calculated. We also calculated the mean power frequency (MPF) and the maximum frequency containing 80 % of the power spectral density (*F80*) of the COPap signal. Measures of frequency were only extracted from COPap due to the fact that the muscles recorded act mostly to move the body's COP in the anterior–posterior direction. Computational methods regarding these variables followed the procedures described by Duarte and Freitas (2010). In summary, the variable *Area* was estimated by fitting an ellipse to the COP set of coordinates (COPap vs. COPml) by means of principal component analysis where the two main axes of the ellipse were found from the resulting eigenvalues of the covariance matrix between COPap and COPml. The length of both axes was optimized to include 95 % of the COP coordinates. The variable *Range* was computed separately for COPap and COPml signals by subtracting the largest and smallest coordinate values recorded in a single trial. *Mean velocities* were also computed separately for COPap and COPml. This variable was estimated by computing the average displacement calculated between recorded samples. *MPF* and *F80* were obtained by first computing the periodogram for the COPap signal (Welch's method and 0.033 Hz resolution) and, based on this periodogram, the frequency band containing 50 and 80 % of the spectral power were recognized (*MPF and F80,* respectively).

Three parametric tests were used to test the possible effect of vision impairment on these variables. Specifically, a one-way ANOVA with factor *Vision* (OEs and CE) was performed on variable *Area*; a two-way MANOVA with factors *Vision* (OEs and CE) and *Direction* (COPap and COPml) on variables *Range* and *Mean Velocity;* and a one-way MANOVA was performed with factor *Vision* (OEs and CE) on variables *MPF and F80.*

Time domain analysis of EMG signals

EMG signals recorded from all six muscles were submitted to two time domain analyses. The first analysis quantified

the relative *amplitude of activation* of each muscle during the execution of OEs and CEs trials by computing a relative index of muscle activation (*IEMG*) as follows. First, EMG signals from OEs and CEs trials were visually inspected to verify the presence of any signal artifacts. The signals recorded were then filtered (20-Hz high-pass, second-order, zero-lag Butterworth filter) and full-wave rectified. Each signal from CE trials was integrated over its trial length and normalized by similar integrals performed on EMG signals from OEs trials. This analysis was used to confirm that all muscles recorded had comparable magnitude of activation across the execution of the two experimental conditions.

The second analysis quantified the *patterns of multi-muscle activation* that participants utilized during CE. This analysis was performed by a vectorial comparison run separately for the anterior and posterior group of muscles (TA, RF, RA and SOL, BF, ERE, respectively). This step was to assure that all participants used similar patterns of muscle activation in both experimental conditions. To this end, we determined the degree of similarity between patterns of muscle activation based on the cosine of the angle between pairs of muscle activation patterns vectors obtained for OEs and CEs trials. These vectors were assembled using the normalized *IEMGs* (Poston et al. 2010; Danna-dos-Santos et al. 2007, 2010, 2014). The cosine of the angle between-pairs of vectors quantifies the degree of similarity in their spatial orientation from 0 to 1, where the former indicates perpendicularity (dissimilarity) and the latter indicates parallelism (similarity). More specifically, values closer to 1 indicate more similar activation patterns during the execution of the two experimental conditions.

Frequency domain analysis of EMG signals

EMG signals were analyzed in the frequency domain by computing estimations of *intermuscular coherence* (EMG–EMG coherence; Grosse et al. 2002) between muscle pairs separately (single-pair estimations) and combined (pooled estimations). Intermuscular coherence was estimated using rectified EMG. Experimental and computational studies have shown that rectified EMG is optimal for assessing intermuscular coherence at low force levels (Boonstra and Breakspear 2012; Farina et al. 2013; Ward et al. 2013), as required during quiet standing. All analyzes were performed following similar procedures reported by Poston et al. (2010). One important aspect of the experimental design was to ensure our investigation followed the functional relationship of the muscles recorded, more specifically those muscles forming both posterior and anterior M-modes. In order to emphasize the functional role of the distribution of common neural inputs, we also computed intermuscular coherence from pairs of EMG signals recorded from muscles with no synergistic relation (*mixed group*, Table 1). It is the inclusion of these muscle pairs that allowed us to support our claim that common neural inputs are (1) involved in the formation of multi-muscle synergistic groups and (2) these groups are formed according to their functionality in controlling the anterior and posterior oscillatory body movements. These claims can only be made in case we compare quantities obtained from the anterior and posterior groups to a group formed by the combination of muscles not as mechanically effective to the execution of the motor task (in our case the mixed group).

Table 1 Averages and standard deviation across participants of postural behavior variables (area, range, *MV* mean velocity, *MPF* mean frequency power, and F80-maximum frequency containing (80 % of the power spectral density) extracted from the COP coordinates in anterior–posterior and medial–lateral directions (COPap and COPml, respectively) under opened-eye (OEs) and closed-eye (CEs) conditions

	Muscle pair	Relationship
1	SOL–BF	Posterior
2	SOL–ERE	Posterior
3	BF–ERE	Posterior
4	TA–RF	Anterior
5	TA–RF	Anterior
6	RF–RA	Anterior
7	SOL–RF	Mixed
8	SOL–RA	Mixed
9	BF–TA	Mixed
10	BF–RA	Mixed
11	ERE–TA	Mixed
12	ERE–RF	Mixed

We did not include any *mixed* pairs of antagonists acting upon the same joint(s) (SOL/TA, BF/RF, and ERE/RA). Agonist/antagonist pairs are recognized for their levels of coupling between EMG signals (Hansen et al. 2002), and they would interfere with our goal of comparing the strength of the correlated neural inputs between signals obtained from muscles forming the anterior and posterior synergist groups and those pairs of non-synergistic muscles (*mixed* group). Agonist/antagonist pairs are the focus of a separate investigation.

Single-pair estimations

Rectified EMG signals from the two trials collected under each experimental condition were concatenated to create a single time series (60 s; 72,000 data points). Concatenation is a standard procedure used to increase the reliability of coherence estimation (Amjad et al. 1997; Maris et al. 2007; Poston et al. 2010), and intermuscular coherence was estimated for pairs of EMG signals by normalizing the cross-spectrum of two EMG signals (fxy) squared by the product of the auto-spectrum of each signal (fxx and fyy) at each frequency (λ):

$$\left|R_{xy}(\lambda)\right|^2 = \frac{\left|f_{xy}(\lambda)\right|^2}{\left|f_{xx}(\lambda)f_{yy}(\lambda)\right|} \quad (1)$$

Intermuscular coherence estimates were obtained from non-overlapping 1-s data segments (i.e., 1,200 samples per segment), resulting in a frequency resolution of 1 Hz. The frequency range analyzed in this study was bounded from 0 to 55 Hz and coherence estimates were considered statistically significant when they exceeded the confidence limit of the null distribution, as proposed by Rosenberg et al. (1989). The confidence limit at $\alpha = 0.05$ and for the number of disjoint segments (L) was determined by

$$Sig(\alpha) = 1 - (1-\alpha)^{\frac{1}{L-1}} \quad (2)$$

In order to compare coherence estimations across participants and different experimental conditions, all estimates were z-transformed by computing the Fisher transformation of the estimates as proposed by Rosemberg et al. (1989) and Amjad et al. (1997)

$$\tan h^{-1}(x) = 0.5 \cdot \log \frac{1+x}{1-x} \quad (3)$$

where x is the coherence estimate.

Analysis of the frequency distribution of correlated neural inputs was achieved by identifying frequency intervals showing significant coherence. The frequency intervals of interest used for further analysis were determined by the frequency intervals showing significant coherence. Quantification of the strength of correlated neural inputs was achieved by computing the integrals within the frequency intervals of interest. These integrals were obtained after all estimates were transformed into z-scores.

Three parametric tests were used to test the possible effect of vision impairment to the strength of correlated neural inputs for the posterior and anterior muscle pairs separately. Specifically, a two-way ANOVA with factors *Vision* (OEs and CE) and *Muscle Pair* (SOL/BF, SOL/ERE, and BF/ERE) and variable *Integral* (integral computed on coherence estimation profiles within 1–10 Hz range) was used for posterior muscle pairs. A similar ANOVA was employed only for the anterior muscle pairs (TA/RF, RF/RA, and TA/RA). Due to the effects found for RF/RA (see "Results"), a third two-way ANOVA was employed with factors *Vision* (OEs and CEs) and *Muscle Pair* (TA/RF and TA/RA) and the same variable *Integral*.

Pooled coherence estimations

Three pooled coherence analyses were performed separately. The first included the three pairs of posterior muscles (SOL/BF, SOL/ERE, and BF/ERE—posterior group; see Table 1). The second analysis included the three pairs of anterior muscles (TA/RF, TA/RA, and RF/RA—anterior group). The third analysis included all six pairs formed by one posterior and one anterior muscle (mixed group). Pooled coherence estimates are considered a weighted average of individual coherence estimates and can be used to increase statistical power. That is, we assume that all muscles forming a single muscle mode share the same neural inputs. Estimates of pooled coherence were obtained as proposed by Amjad et al. (1997):

$$\frac{\left|\sum_{i=1}^{k} f_{xy}(\lambda)L_i\right|^2}{\left(\left(\sum_{i=1}^{k} f_{xx}(\lambda)L_i\right)\left(\sum_{i=1}^{k} f_{yy}(\lambda)L_i\right)\right)} \quad (4)$$

Analysis of the frequency distribution and strength of correlated neural inputs obtained from pooled coherence calculations were also based on the determination of frequency bands of interest and the calculation of integrals within these frequency bands. To test the possible effect of vision impairment to these integrals and among the three muscle groupings mentioned (posterior, anterior, and mixed), a two-way ANOVA with factors *Vision* (OEs, CEs) and *Muscle Grouping* (Posterior, Anterior, and Mixed) was performed on the variable *Integral*. All parametric tests mentioned were performed keeping levels of significance at 5 % ($\alpha = 0.05$). All tests were performed by the IBM SPSS statistics software suite (version 20, IBM® SPSS).

Results

COP behavior: general features

In general, the COP of all participants oscillated more and faster in the closed-eye (CE) condition. Figure 1 exemplifies this observation by showing the COPap (anterior–posterior coordinates) and COPml (medial–lateral coordinates) profiles recorded from a representative participant during the execution of OEs (Panels A and B) and CEs trials (Panels C and D). Table 2 summarizes the averages and SD across participants computed for all seven COP variables. The values reported in this table show the changes caused by the absence of visual inputs during the execution of the CE trials. More specifically, we found a consistent increase in the average values obtained for the elliptical areas, ranges, and mean velocities of COP coordinates when vision was not available. The lack of visual information also induced changes in the frequency content measures of the COPap signal. Note the increase of both MPF and F80 measures observed for CE trials.

These observations were confirmed statistically. The elliptical area containing 95 % of the COP path profile (*Area*) showed significant increased values during CE trials

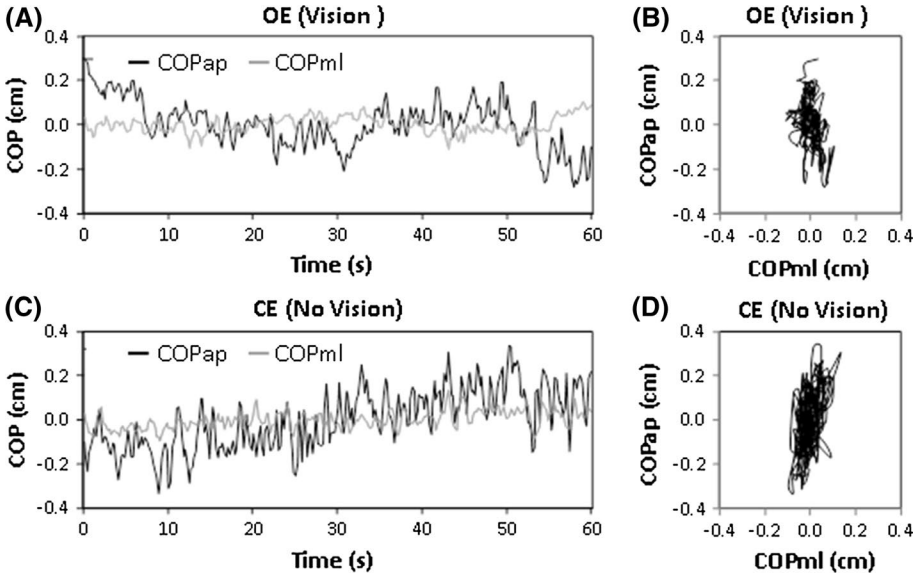

Fig. 1 Profiles of COP coordinates in anterior–posterior (COPap) and medial–lateral (COPml) directions recorded from a representative participant during the execution of OEs (**a**, **b**) and CEs trials (**c**, **d**) trials. *Black* and *gray lines* in (**a**) and **c** represent COPap and COPml, respectively. **b**, **d** The same coordinates on a *xy* plot where one can note the enlarged area travelled by the COP during the execution of a CEs trial (**d**) when compared to an OEs trial (**b**)

Table 2 Organization of muscle pairs submitted to the intermuscular coherence analyses (pooled, and single pair)

	Area (cm^2)	Range COPap (cm)	Range COPml (cm)	MV COPap (cm/s)	MV COPml (cm/s)	MPF COPap (Hz)	F80 COPap (Hz)
OE (vision)	1.14 ± 0.32	2.08 ± 0.71	1.00 ± 0.38	0.70 ± 0.20	0.43 ± 0.15	0.23 ± 0.07	0.34 ± 0.19
CE (no vision)	1.65 ± 0.55	2.22 ± 0.43	1.33 ± 0.42	1.07 ± 0.30	0.45 ± 0.14	0.34 ± 0.09	0.51 ± 0.20

SOL soleus, *BF* biceps femoris, *ERE* lumbar erector spinae, *TA* tibialis anterior, *RF* rectus femoris, *RA* rectus abdominis

[$F_{(1,16)} = 6.550$, $p = 0.021$]. Increased values of COP mean velocities during CE trials were confirmed by the two-way MANOVA for the variables *Range* and *Mean Velocity* [*Vision* $F_{(2,31)} = 3.584$, Wilks' $\lambda = 0.812$, $p = 0.040$; *Direction* $F_{(2,31)} = 25.849$, Wilks' $\lambda = 0.375$, $p < 0.001$] without significant interactions [*Vision* × *Direction* $F_{(2,31)} = 3.264$, Wilks' $\lambda = 0.8263$, $p = 0.052$]. Follow-up univariate analyses confirmed significantly larger values of *Mean Velocities* but not *Range* during CE trials [$F_{(1,32)} = 0.342$, $p = 0.014$ and $F_{(1,32)} = 0.258$, $p = 0.615$, respectively].

In addition, the one-way MANOVA confirmed a significant effect of the factor *Vision* [$F_{(2,15)} = 4.483$, Wilks' $\lambda = 0.626$, $p = 0.030$]. Follow-up univariate analyses confirmed significantly larger values of *MPF* but not *F80* during CE trials [$F_{(1,16)} = 8.257$, $p = 0.011$ and $F_{(1,16)} = 3.271$, $p = 0.089$, respectively].

Muscle activation: time domain analysis

As expected, all participants performed both visual conditions with ease. They also used similar muscle activation levels across the two experimental conditions. Figure 2a shows the rectified EMG recordings for all six muscles obtained from a representative participant during the execution of OEs (left column) and CEs trials (right column). Figure 2b shows the average across subjects for *IEMG* indices. The observed averages for *IEMG* were close to 1 and confirm that participants generally employed similar magnitudes of activation in both conditions (this measure describes a ratio between the integrals of EMG signals recorded during OEs and CEs). Participants also employed comparable patterns of muscle activation in both experimental conditions as shown by the vector analysis that revealed large cosine values across participants with very little deviation (posterior group = 0.979 ± 0.022 and anterior group = 0.971 ± 0.057).

Muscle activation: frequency domain analysis

Pooled coherence

Figure 3a shows average pooled coherence across participants computed across the three muscles pairs formed between SOL, BF, and ERE in the OEs and CEs conditions (black and gray traces, respectively). Pooled coherence was significant within the frequency interval of 1–10 Hz during the execution of OEs trials, and a considerable drop in coherence was observed in the CE condition. Based on this finding, the frequency of interest was determined between 1 and 10 Hz. A similar effect was found for the estimates

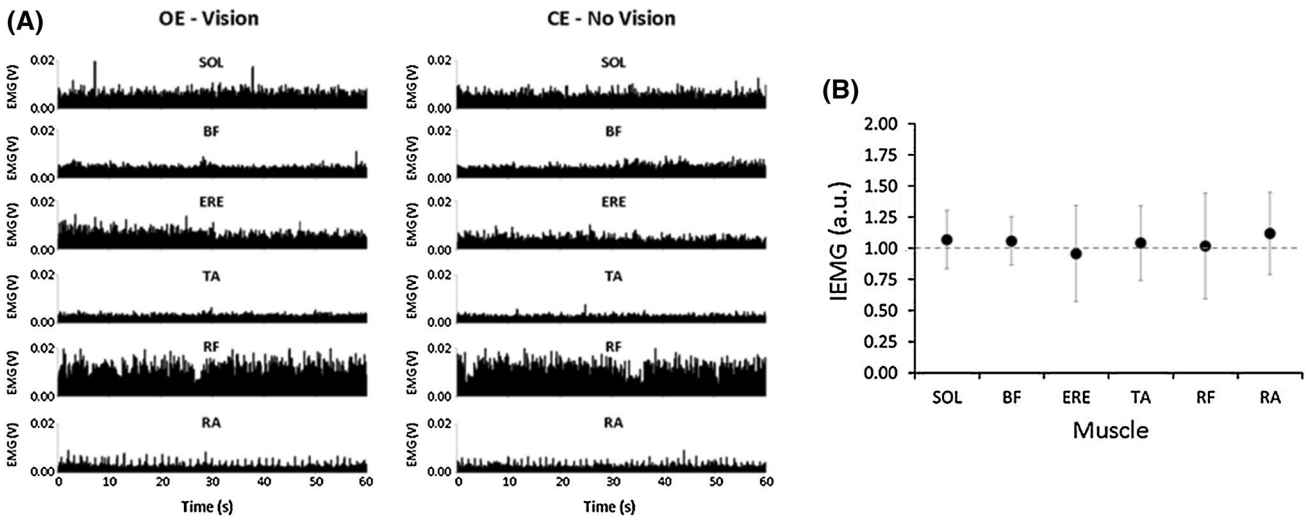

Fig. 2 **a** Set of concatenated and rectified EMG signals of six muscles (*SOL* soleus, *BF* biceps femoris, *ERE* lumbar erector spinae, *TA* tibialis anterior, *RF* rectus femoris, and *RA* rectus abdominis) recorded from a representative participant during the execution of opened-eye (OEs, on the *left*) and closed-eye (CEs, on the *right*) trials. **b** Averages and SD across participants of the variable *IEMG*. *Dashed line* indicates the region of the graph where the relative levels of muscle activation would be equal between OEs and CEs trials. Note that values around this line confirm similar muscle activation levels for all six muscles during the execution of OEs and CEs trials

calculated across the signals recorded from the anterior muscle pairs (Fig. 3b). Results for the pooled coherence analysis performed for muscle pairs formed by one posterior and one anterior muscle (*mixed* group) are shown in Fig. 3c. Note that in contrast to the posterior and anterior M-modes, no significant intermuscular coherence was observed across all frequencies. The averages and SD across participants for the integrals calculated for the frequency band of interest are displayed in Fig. 4.

Reduced common neural inputs in the CE condition (observed for the anterior and posterior muscle pairs) was confirmed statistically [*Vision* $F_{(1,48)} = 11.958$, $p = 0.001$; *Muscle Grouping* $F_{(2,48)} = 11.448$, $p = 0.000$]. The interaction of these two factors was significant [$F_{(2,48)} = 2.875$, $p = 0.066$]. Follow-up Tukey's pair-wise comparisons confirmed significantly higher coherence for anterior and posterior muscle groups compared with the mixed group ($p < 0.0005$ and $p = 0.017$, respectively). Since no significant coherence was observed for the *mixed* group of EMG signals, only the results for the posterior and anterior groups are presented in the following section.

Single-pair coherence (posterior group)

Figure 5 (Panels A, C, and E) shows the average intermuscular coherence spectra for each muscle pair (SOL/BF, SOL/ERE, and BF/ERE) within the frequency range of 0–55 Hz. Single-pair estimates revealed significant coherence within the 1- to 10-Hz frequency interval during OEs condition. Similar to the pooled coherence estimates, the single-pair estimates for all three posterior muscle pairs revealed a significant decrease in coherence in the CE condition. The averages and SD across participants for the integrals computed for these muscle pairs are shown in Fig. 6a. These observations were corroborated by the two-way ANOVA that showed a significant effect of *Vision* [$F_{(1,48)} = 6.796$, $p = 0.012$], but not for *Muscle Pair* [$F_{(2,48)} = 2.600$, $p = 0.085$]. Note that even though integrals values for the BF/ERE pair under both OEs and CEs conditions were higher when compared to the integrals for the other two muscle pairs, they were not statistically significant ($p = 0.085$). No significant interaction effect between *Vision* and *Muscle Pair* was observed [$F_{(2,48)} = 0.105$, $p = 0.900$].

Single-pair coherence (anterior group)

Figure 5 (Panels B, D, and F) shows average intermuscular coherence for each pair of anterior muscles (TA/RF, TA/RA, and RF/RA). Similar to the results of the posterior group, estimates for these muscle pairs revealed significant values within the frequency interval of 1–10 Hz in the OEs condition and a significant decrease in the CE condition. However, differently from the posterior group, one of the muscle pairs failed to reach significant values of coherence (RF/RA, panel F). The averages and SD across participants for the integrals computed for the OEs and CEs conditions are shown in Fig. 6b. The designated test for this comparison showed no significant effect of *Vision* [$F_{(1,48)} = 3.618$, $p = 0.063$], but it did for *Muscle*

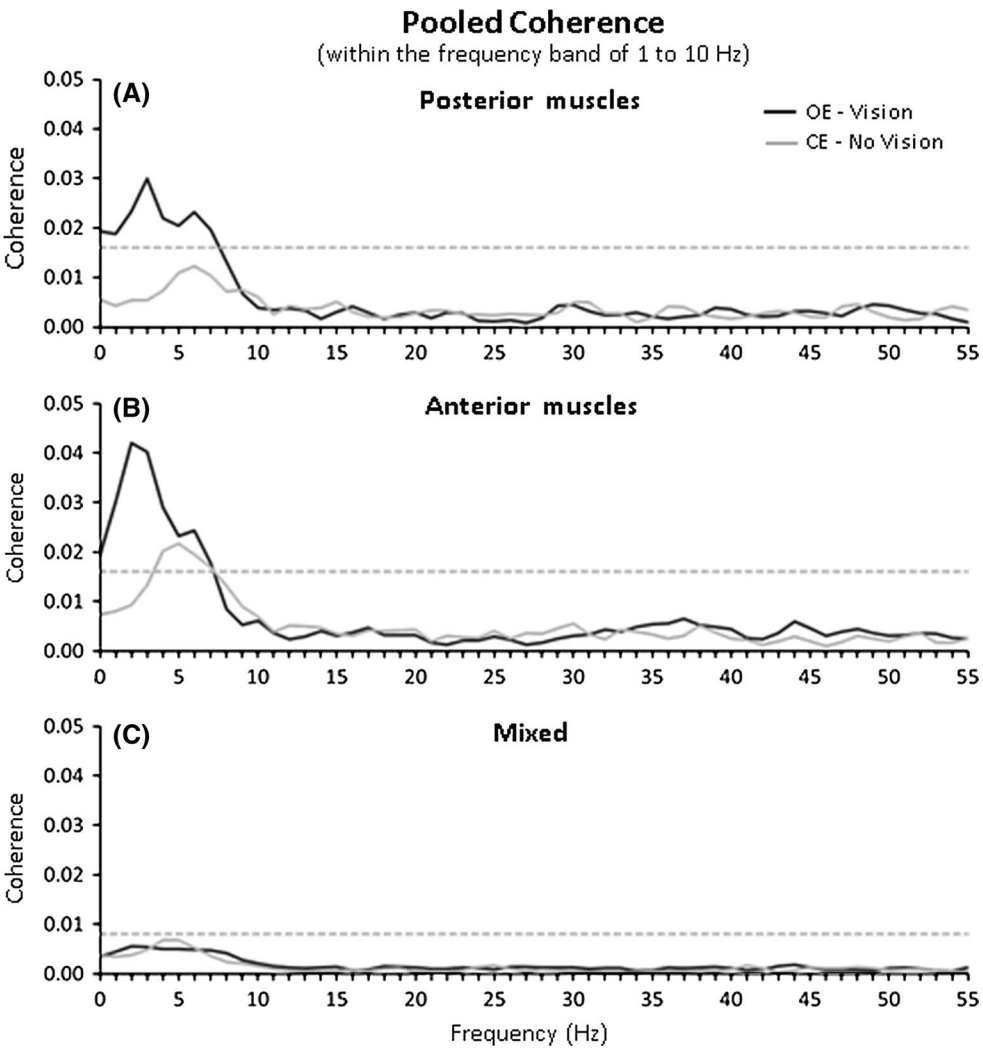

Fig. 3 **a** Averages across participants of the pooled coherence (expressed in *z*-scored pooled coherence profiles) obtained for all pairs formed between posterior muscles (*SOL* soleus, *BF* biceps femoris, and *ERE* erector spinae) during the execution of opened-eye (OEs, in *black line*) and closed-eye (CEs, in *gray line*) conditions. *Dotted gray line* depicts the 95 % confidence level. Note that the area of the profile between 0 and 10 Hz was consistently above the line of confidence for OEs and therefore was considered significant. Based on this observation, the integrals of the same interval were computed, normalized, and compared with each other. **b** Averages across participants of the pooled coherence (expressed in *z*-scored pooled coherence profiles) obtained for all pairs formed between anterior muscles (*TA* tibialis anterior, *RF* rectus femoris, and *RA* rectus abdominis). **c** Averages across participants of the pooled coherence (expressed in *z*-scored pooled coherence profiles) obtained for all pairs formed between one anterior and one posterior muscle (pairs are described in Table 1)

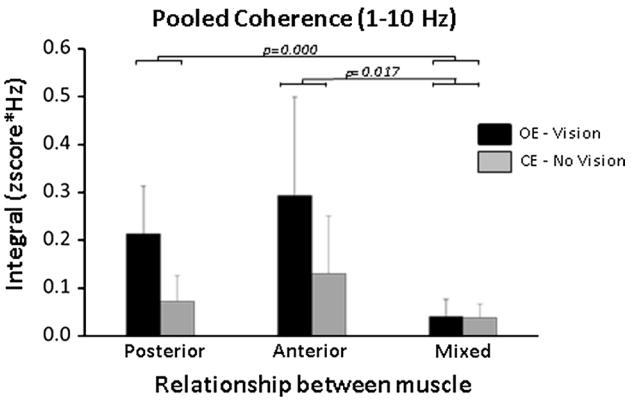

Fig. 4 Averages and SD across participants of pooled coherence estimate integrals computed over the frequency interval of 1–10 Hz for muscle pairs formed by either only posterior muscles (Posterior), or only anterior muscles (Anterior), or one anterior and one posterior muscle (mixed) during the execution of opened-eye (OEs, in *black bars*) and closed-eye (CEs, in *gray bars*) conditions

Pair [$F_{(2,48)} = 4.491$, $p = 0.016$]. A follow-up Tukey's pairwise comparison revealed a significant difference between the integrals obtained for TA/RF and RF/RA ($p = 0.013$). We believe that the lack of a significant effect of *Vision* was caused by including the muscle pair RF/RA into this analysis. Therefore, the second two-way ANOVA run excluding the RF/RA data confirmed a significant effect of *Vision* [$F_{(1,32)} = 4.468$, $p = 0.042$], but not for *Muscle Pair* [$F_{(1,32)} = 0.794$, $p = 0.380$]; no significant interaction effect was observed [$F_{(1,32)} = 0.055$, $p = 0.816$].

Discussion

This study confirmed the presence of common neural input to postural muscles forming synergies intended to control bipedal quiet stance. Specifically, a group formed by the posterior muscles SOL, BF, and ERE and a group

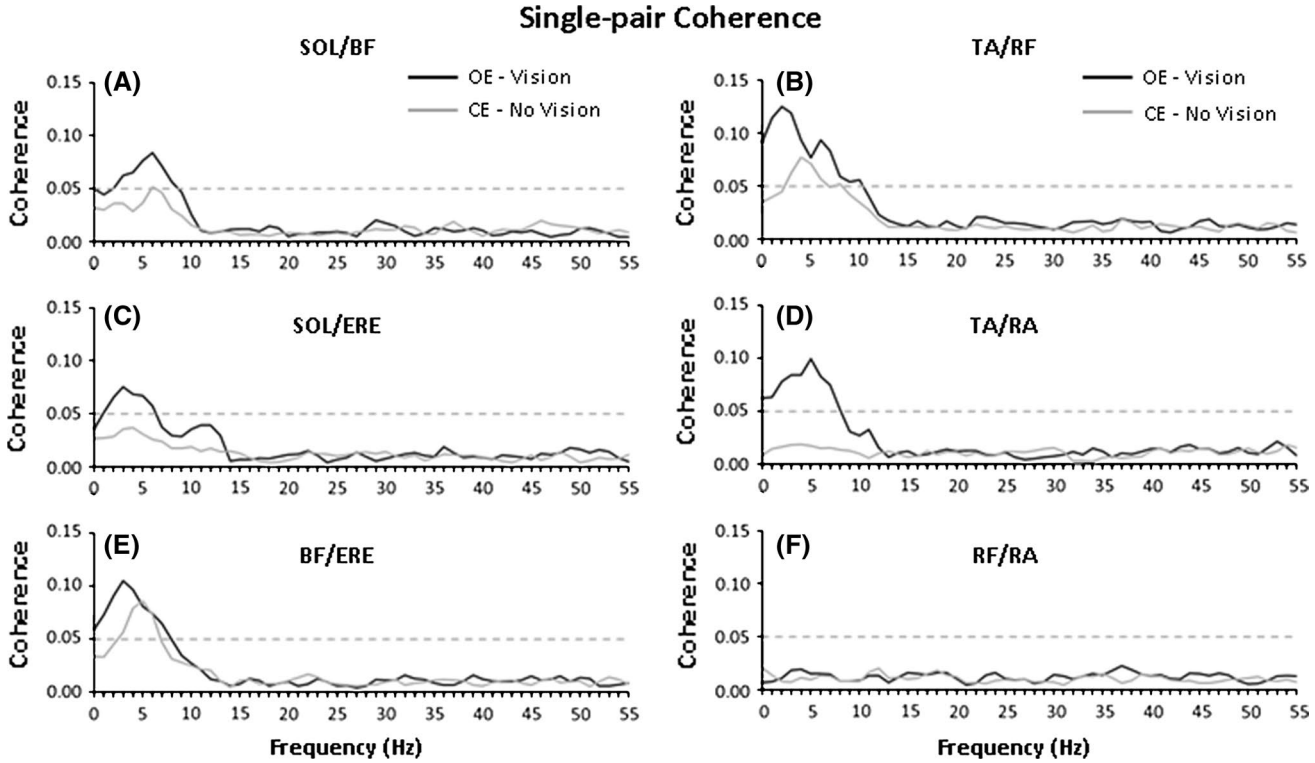

Fig. 5 **a**, **c**, **d** Averages across participants of the intermuscular coherence (expressed in *z*-scored single-pair coherence profiles) obtained separately for each pair of posterior muscles (SOL/BF, SOL/ERE and BF/ERE) during the execution of opened-eye (OEs, in *black line*) and closed-eye (CEs, in *gray line*) conditions. **b** Averages across participants of the intermuscular coherence (expressed in *z*-scored single-pair coherence profiles) obtained separately for each pair of anterior muscles (TA/RF, TA/RA and RF/RA) during the execution of opened-eye (OEs, in *black line*) and closed-eye (CEs, in *gray line*) conditions. On both panels *dashed gray line* notes the confidence level for no significant intermuscular coherence

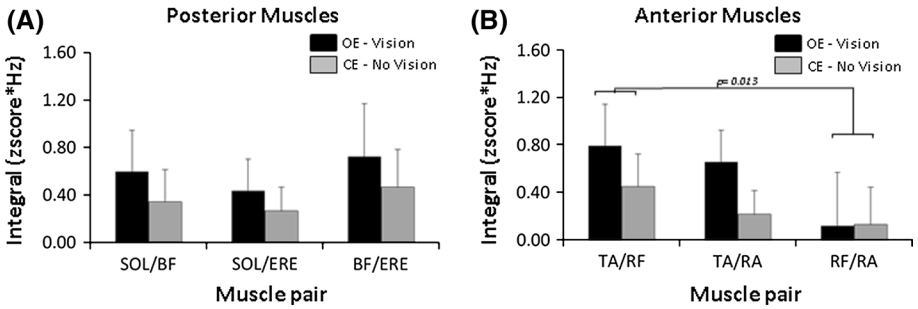

Fig. 6 **a** Averages and SD across participants of single-pair estimate integrals computed over the frequency interval of 1–10 Hz for all three posterior muscle pairs (SOL/BF, SOL/ERE and BF/ERE) during the execution of opened-eye (OEs, in *black bars*) and closed-eye (CEs, in *gray bars*) conditions. *Note* The significantly smaller area obtained for all pairs under the execution of CEs experimental condition. **b** Averages and SD across participants of single-pair estimate integrals computed over the frequency interval of 1–10 Hz for all three anterior muscle pairs (TA/RF, TA/RA and RF/RA) during the execution of opened-eye (OEs, in *black bars*) and closed-eye (CEs, in *gray bars*) conditions. *Note* The significantly smaller area obtained for two pairs (TA/RF and TA/RA) under the execution of CEs experimental condition

formed by the anterior muscles TA, RF, and RA showed significantly stronger coherence compared with a set of EMG signals formed by a mix of anterior and posterior muscles (considered here as non-synergistic). Significant intermuscular coherence was only observed within a frequency interval of 1–10 Hz and a significant decrease in intermuscular coherence when the same task was performed in the absence of vision, confirming the hypothesis

that a short-term interruption of visual input affects the generation of common neural inputs. Following, we discuss our findings and their implications to the multi-muscle control of bipedal stance.

Control of the human's bipedal stance requires the coordination of multiple muscles with temporal, spatial, and magnitude precision. However, due to the large number of muscles involved, upright stance can be achieved by a large number of combinations of muscular outputs. This redundancy, while allowing flexibility to perform a motor action, also mandates that the CNS masters the very many degrees of freedom (Turvey 1990). Many have suggested that in order to deal with this large number of variables, the CNS unites these elements according to their function and then controls them in a synergistic and goal-directed fashion (Scholz and Schöner 1999; Gelfand and Latash 2002). According to this perspective, motor control reflects a hierarchy where the lower primary level represents the formation of these groups, while a higher secondary level represents a stage where these newly created groups are used as control elements. This notion of synergies has been used with respect to the control of movement in a variety of species ranging from spinal frogs, to cats, and humans (d'Avella et al. 2003). Several approaches and techniques have emerged to capture possible patterns of muscle activations and their role regarding the dynamics of a certain action. For example, the framework of the uncontrolled manifold hypothesis (UCM) was developed from the principle of motor abundance proposed by Gelfand and Latash (2002) and aimed to provide an operational method to recognize and quantify multi-elements synergies (Scholz and Schöner 1999). This approach has been used to investigate multi-muscle synergies involved in the task of standing up (Krishnamurthy et al. 2003a, b). Results revealed that a set of synergistic groups were consistently activated; among them, a posterior group is formed by muscles spanning across several major joints (ankle, knee, hip, and intervertebral joints), with the purpose of swaying the body backwards around the ankle joint (hence the nomenclature push-backward or posterior muscle mode—M-mode). A second group of muscles is formed by anterior muscles also crossing major joints but with the ability to sway the body forward. These investigations also provided evidence that the activation of such muscle modes co-vary to allow a stable trajectory of the body COP. Other investigations provided evidence that this synergistic organization changes according to the challenges imposed by the task (Danna-dos-Santos et al. 2008), and suggest that the CNS optimizes its controlling mechanisms according to the imposed task requirements. These studies, however, were not designed to identify the neural mechanisms involved in the generation of such synergies. Our study has provided this additional step by providing initial evidence, indicating that their formation is driven by common input to different muscles.

In this present study, we aimed to examine a possible neural mechanism involved in the formation of these two synergistic groups (push-back and push-forward M-modes) by means of intermuscular coherence. More specifically, we investigated the hypothesis that correlated neural inputs may be a mechanism used to assemble these synergistic groups. The present results support the notion of correlated neural inputs during quiet stance as revealed by significant intermuscular coherence found within the frequency interval of 1–10 Hz among posterior and anterior synergistic muscles. Synchronization of EMG signals within this frequency interval (<10 Hz) is consistent with previous studies that reported similar findings during the execution of slow movements (Kamen and DeLuca 1992; Vallbo and Wessberg 1993; Farmer et al. 1993; DeLuca and Erim 2002). In fact, similar results have been recently reported by us (Danna-dos-Santos et al. 2014). In that study, we reported synchronizations that were not only concentrated between 1 and 10 Hz but also extended to frequencies up to 20 Hz. We believe that the major factor influencing these results is related to the type of task performed by the participants. More specifically, in this present study our participants stood up freely, while the participants in our previous study were standing under an induced isometric contraction of all muscles evaluated. Changes in intermuscular synchronizations as a function of the type of contraction and the appearance of multiple significant frequency bands have been reported by several studies, and they seem to point to changes on the neural mechanisms used to generate the motor outputs that are task specific (Farmer et al. 1993; MacAuley et al. 1997; Mima et al. 2000; Grosse et al. 2002).

The neural sites responsible for the generation of such common input remain unclear, and multiple origins have been proposed in the literature. For example, Farmer et al. (1993) studied stroke survivors with damage to motor cortical areas and showed that despite cortical damage, intermuscular coherence was still present within the frequency interval of 1–12 Hz, suggesting that synchronization within this frequency interval was unlikely to originate within the motor cortex. Boonstra et al. (2009b) also showed that intermuscular coherence at 7–13 Hz between bilateral hand muscles was not synchronized with cortical activity, further supporting a sub-cortical origin of intermuscular coherence in the lower frequency band. In contrast, the collective results of Mima and colleagues (Mima and Hallett 1999; Mima et al. 2000, 2001) have not only reported significant values of corticomuscular coherence within the frequency interval of 3–13 Hz for hand muscles, but they also extended this finding to other muscles such as the biceps brachii and abductor hallucis (intrinsic muscle of the foot). According to Mima et al. (2000), synchronizations in this lower frequency band likely reflect the involvement of the

inferior olive and the thalamic cortical loop as the possible sources or formation of synchronizations found between 3 and 13 Hz.

The strength of correlated neural inputs was similar across five of the six primary muscle pairs (all three posterior muscles pairs and two anterior muscle pairs). This is an interesting finding since within each muscle group these muscle pairs have distinct anatomical relations: The SOL/BF and TA/RF muscle pairs are formed by two adjacent muscles placed relatively more distally, whereas BF/ERE and RF/RA are muscle pairs formed by adjacent muscles placed more proximally; and the SOL/ERE and RF/RA are muscle pairs formed by one proximal and one distal muscle. This finding suggests that under the experimental circumstances investigated here, the M-modes are likely formed based on their functional role of moving the body either backward of forward, rather than based on their anatomical location. In addition, similar previous studies have shown evidence for common drive only present between pairs of muscles that share a common joint complex (e.g., Gibbs et al. 1995). The functional role of the distribution of common neural inputs is also supported by the results showing no significant values of intermuscular coherence for those signals recorded from pairs of non-synergistic muscles (mixed group). These mixed pairs were formed by one anterior and one posterior muscle, and the lack of synchrony between them suggests that only muscles that are able to effectively control body oscillation in the anterior–posterior direction receive common neural inputs. This finding corroborates with the notion that the formation of synergistic muscle groups is task specific (Latash 2008). In the case of a quiet standing where most of the oscillatory body movement happens around the ankle joint (i.e., ankle-strategy), it is expected that muscles placed on either the anterior or posterior aspects of the axial skeleton are most effective in controlling body movements in the anterior–posterior direction. The activation of a mixed pair is not as mechanically effective to counteract movements around the ankle joint during quiet standing. Therefore, it is expected that the CNS will elicit the activation of muscle groups that are mechanically effective for the accomplishment of the task.

Moreover, the frequency profiles of common input were similar for the posterior and anterior muscle groups and hence may suggest that the posterior and anterior muscle groups received the same common input. However, intermuscular coherence was calculated across all time points and hence while the intermuscular coherence spectra had a similar frequency profile, the posterior and interior muscle groups may have received common input at different points in time (e.g., when the body is swaying either backward or forward). Indeed, Boonstra et al. (2009a) showed that bilateral TA muscles receive common 10 Hz input only in the most posterior position when swaying in anterior–posterior direction.

We found that intermuscular coherence decreased significantly when participants were asked to stand with eyes closed (EC condition), suggesting that visual information plays an important role in the formation of postural synergies during bipedal stance. Previous studies have shown mixed effects of the removal of visual information on intermuscular coherence. Boonstra et al. (2008) reported an increase in intermuscular coherence within the frequency band of 0–5 Hz between bilateral lower leg muscles (SOL and gastrocnemius) during the execution of quiet stance in the absence of visual inputs. In contrast, (Mochizuki et al. 2007) showed that common input to individual MUs of bilateral SOL muscles did not differ between standing with eyes opened or closed. The opposite effects on intra-limb and inter-limb coherence may reflect a change in the control strategy after removing visual information, that is, the postural control strategy may depend more on proprioceptive information from the ankle joint in the absence of vision (cf. Saffer et al. 2008). Consequently, changes in the availability of visual inputs change the organization of neural drive to synergistic muscles involved in postural control. While visual information appears to play an important role in the generation of common input, future studies investigating both intra- and inter-limb coherence are required to map the reorganization in common input after removing visual information.

Conclusions

We found that the coordination of postural muscles likely involve the distribution of common neural inputs to distinct muscles in order to form modal units that can be manipulated by the CNS. The synchronization patterns observed between muscle pairs (pooled and separately) were found to be concentrated within a frequency interval of 1–10 Hz. The synchronizations reported showed similar strength among six postural muscles and have been interpreted as a sign of a common neural drive underlying multi-muscle control. In addition, our results suggest that postural M-modes are likely formed based on their functional role of moving the body either backward of forward, rather than based on their anatomical location. We also found that the lack of vision during the execution of quiet stance task results in (1) a change to this drive and (2) this change affects all components of this synergistic group. These results indicate a key role of visual information in the generation of common input to muscles involved in postural control.

Acknowledgments The authors would like to acknowledge the School of Physical Therapy and Rehabilitation Science for funding and supporting this study. Dr Boonstra acknowledges support from the Veni Fellowship from the Netherlands Organization for Scientific Research (NWO No. 45110-030).

References

Allum JH, Pfaltz CR (1985) Visual and vestibular contributions to pitch sway stabilization in the ankle muscles of normals and patients with bilateral peripheral vestibular deficits. Exp Brain Res 58:82–94

Amjad AM, Halliday DM, Rosenberg JR, Conway BA (1997) An extended difference of coherence test for comparing and combining several independent coherence estimates: theory and application to the study of motor units and physiological tremor. J Neurosci Methods 73:69–79

Barela JA, Weigelt M, Polastri PF, Godoi D, Aguiar SA, Jeka JJ (2014) Explicit and implicit knowledge of environment states induce adaptation in postural control. Neurosci Lett 566:6–10

Bernstein N (1967) The coordination and regulation of movements. Pergamon, London, p 196

Boonstra TW, Breakspear M (2012) Neural mechanisms of intermuscular coherence: implications for the rectification of surface electromyography. J Neurophysiol 107:796–807

Boonstra TW, Roerdink M, Daffertshofer A, Vugt B, Werven G, Beek PJ (2008) Low-alcohol doses reduce common 10-to 15-Hz input to bilateral leg muscles during quiet standing. J Neurophysiol 100(Pt 4):2158–2164

Boonstra TW, Daffertshofer A, Roerdink M, Flipse I, Groenewoud K, Beek PJ (2009a) Bilateral motor unit synchronization of leg muscles during a simple dynamic balance task. Eur J Neurosci 29(3):613–622

Boonstra TW, van Wijk BCM, Praamstra P, Daffertshofer A (2009b) Corticomuscular and bilateral EMG coherence reflect distinct aspects of neural synchronization. Neurosci Lett 463:17–21

Criswell E (2010) Cram's introduction to surface electromyography, 2nd edn. Jones and Bartlett Learning, USA, p 412

Danna-dos-Santos A, Slomka K, Latash ML, Zatsiorsky VM (2007) Muscle modes and synergies during voluntary body sway. Exp Brain Res 179:533–550

Danna-dos-Santos A, Degani AM, Latash ML (2008) Flexible muscle modes and synergies in challenging whole-body tasks. Exp Brain Res 189:171–187

Danna-dos-Santos A, Shapkova EY, Shapkova AL, Degani AM, Latash ML (2009) Postural control during upper body locomotor-like movements: similar synergies based on dissimilar muscle modes. Exp Brain Res 193:568–579

Danna-dos-Santos A, Poston B, Jesunathadas M, Bobich LR, Hamm T, Santello M (2010) Influence of fatigue on hand muscle coordination and EMG–EMG coherence during three-digit grasping. J Neurophysiol 104:3576–3587

Danna-dos-Santos A, Boonstra TW, Degani AM, Cardoso VS, Magalhaes AT, Mochizuki L, Leonard CT (2014) Multi-muscle control during bipedal stance: an EMG-EMG analysis approach. Exp Brain Res 232(1):75–87

d'Avella A, Saltiel P, Bizzi E (2003) Combinations of muscle synergies in the construction of a natural motor behavior. Nat Neurosci 6(3):300–308

DeLuca CJ, Erim Z (2002) Common drive in motor units of a synergistic muscle pair. J Neurophysiol 87:2200–2204

Dijkstra TM, Schöner G, Gielen CC (1994a) Temporal stability of the action-perception cycle for postural control in a moving visual environment. Exp Brain Res 97(3):477–486

Dijkstra TM, Schöner G, Giese MA, Gielen CC (1994b) Frequency dependence of the action-perception cycle for postural control in a moving visual environment: relative phase dynamics. Biol Cybern 71(6):489–501

Duarte M, Freitas SMSF (2010) Revision of posturography based on force plate for balance evaluation. Brazil Physiother J 14(3):183–192

Farina D, Negro F, Jiang N (2013) Identification of common synaptic inputs to motor neurons from the rectified electromyogram. J Physiol 591:2403–2418

Farmer SF, Bremner FD, Halliday DM, Rosenberg JR, Stephens JA (1993) The frequency content of common synaptic inputs to motoneurones studied during voluntary isometric contraction in man. J Physiol 470:127–155

Fitzpatrick RC, Gorman RB, Burke D, Gandevia SC (1992) Postural proprioceptive reflexes in standing human subjects: bandwidth of response and transmission characteristics. J Physiol 458:69–83

Gatev P, Thomas S, Kepple T, Hallett M (1999) Feedforward ankle strategy of balance during the quiet stance in adults. J Physiol 514(3):915–928

Gelfand IM, Latash ML (2002) On the problem of adequate language in biology. In: Latash ML (ed) Progress in motor control, vol 2: Structure-eunction relations in voluntary movement. Human Kinetics, Urbana, IL, pp 209–228

Gibbs J, Harrison LM, Stephens JA (1995) Organization of inputs to motoneurone pools in man. J Physiol 485(1):245–256

Grosse P, Cassidy MJ, Brown P (2002) EEG-EMG, MEG-EMG and EMG-EMG frequency analysis: physiological principles and clinical applications. Clin Neurophysiol 113(10):1523–1531

Hansen S, Hansen NL, Christensen LO, Petersen NT, Nielsen JB (2002) Coupling of antagonistic ankle muscles during co-contraction in humans. Exp Brain Res 146:282–292. doi:10.1007/s00221-002-1152-3

Kamen G, DeLuca CJ (1992) Firing rate interactions among human orbicularis oris motor units. Int J Neurosci 64(1–4):167–175

Krishnamoorthy V, Goodman SR, Latash ML, Zatsiorsky VM (2003a) Muscle synergies during shifts of the center of pressure by standing persons: identification of muscle modes. Biol Cybern 89:152–161

Krishnamoorthy V, Latash ML, Scholz JP, Zatsiorsky VM (2003b) Muscle synergies during shifts of the center of pressure by standing persons. Exp Brain Res 152:281–292

Latash ML (2008) Synergy. Oxford University Press, USA, p 432

Lee DN, Lishman JR (1975) Visual proprioceptive control of stance. J Hum Mov Stud 1:87–95

Maris E, Schoffelen JM, Fries P (2007) Nonparametric statistical testing of coherence differences. J Neurosci Methods 163:161–175

McAuley JH, Rothwell JC, Marsden CD (1997) Frequency peaks of tremor, muscle vibration and electromyographic activity at 10 Hz, 20 Hz and 40 Hz during human finger muscle contraction may reflect rhythmicities of central neural firing. Exp Brain Res 114:525–541

Mima T, Hallett M (1999) Electroencephalographic analysis of cortico-muscular coherence: reference effect, volume conduction and generator mechanism. Clin Neurophysiol 110:1892–1899

Mima T, Steger J, Schulman AE, Gerloff C, Hallett M (2000) Electroencephalographic measurement of motor cortes control of muscle activity in humans. Clin Neurophysiol 111:326–337

Mima T, Matsuoka T, Hallett M (2001) Information flow from the sensorimotor cortex in humans. Clin Neurophysiol 112:122–126

Mochizuki G, Semmler JG, Ivanova TD, Garland SJ (2006) Low-frequency common modulation of soleus motor unit discharge is enhanced during postural control in humans. Exp Brain Res 175:584–595

Mochizuki G, Ivanova TD, Garland SJ (2007) Factors affecting the common modulation of bilateral motor unit discharge in human soleus muscles. J Neurophysiol 97:3917–3925

Polastri PF, Barela JA (2013) Adaptive visual re-weighting in children's postural control. PLoS ONE 8(12):e82215

Poston B, Danna-dos-Santos A, Jesunathadas M, Hamm TM, Santello M (2010) Force-independent distribution of correlated neural inputs to hand muscles during three-digit grasping. J Neurophysiol 104:1141–1154

Rosenberg JR, Amjad AM, Breeze P, Brillinger DR, Halliday DM (1989) The Fourier approach to the identification of functional coupling between neuronal spike trains. Prog Biophys Mol Biol 53:1–31

Saffer M, Kiemel T, Jeka J (2008) Coherence analysis of muscle activity during quiet stance. Exp Brain Res 185(2):215–226

Scholz JP, Schöner G (1999) The uncontrolled manifold concept: identifying control variables for a functional task. Exp Brain Res 126:289–306

Schöner G (1991) Dynamic theory of action-perception patterns: the "moving room" paradigm. Biol Cybern 64(6):455–462

Schumann T, Redfern MS, Furman JM, el-Jaroudi A, Chaparro LF (1995) Time-frequency analysis of postural sway. J Biomech 28:603–607

Simoneau GG, Leibowitz HW, Ulbrecht JS, Tyrrell RA, Cavanagh PR (1992) The effects of visual factors and head orientation on postural steadiness in women 55 to 70 years of age. J Gerontol 47(5):M151–M158

Turvey MT (1990) Coordination. Am Psychol 45(8):938–953

Vallbo AB, Wessberg J (1993) Organization of motor output in slow finger movements in man. J Physiol 469:673–691

Wang Y, Zatsiorsky VM, Latash ML (2005) Muscle synergies involved in shifting the center of pressure while making a first step. Exp Brain Res 167(2):196–210

Ward N, Farmer S, Berthouze L, Halliday D (2013) Rectification of EMG in low force contractions improves detection of motor unit coherence in the beta-frequency band. J Neurophysiol 110:1744–1750

Wood JM, Lacherez PF, Black AA, Cole MH, Boon MY, Kerr GK (2009) Postural stability and gait among older adults with age-related maculopathy. IOVS 50(1):482–487